Interaction of singlet excitons with polarons in wide band-gap organic semiconductors: A quantitative study

E. J. W. List,[1,2,*] C.-H. Kim,[2,3] A. K. Naik,[2,3,4] U. Scherf,[5] G. Leising,[6] W. Graupner,[7,†] and J. Shinar[2,3,4]
[1]*Institut für Festkörperphysik, Technische Universität Graz, A-8010 Graz, Austria*
[2]*Ames Laboratory-USDOE, Iowa State University, Ames, Iowa 50011*
[3]*Department of Physics and Astronomy, Iowa State University, Ames, Iowa 50011*
[4]*Microelectronics Research Center, Iowa State University, Ames, Iowa 50011*
[5]*Institut für Physikalische und Theoretische Chemie, Universität Potsdam, D-14476 Golm, Germany*
[6]*Science & Technology AT&S AG, A-8700 Leoben, Austria*
and Institute of Nanostructured Materials and Photonics, Joanneum Research Inc. A-8160 Weiz, Austria
[7]*Department of Physics, Virginia Tech, Blacksburg, Virginia 24060*
(Received 31 August 2000; published 26 September 2001)

The steady-state photoinduced absorption (PA), photoluminescence (PL), PL-detected magnetic resonance (PLDMR), and PA-detected magnetic resonance (PADMR) of poly- and oligo-(*para*-phenylenes) films is described. In particular, the excitation density (laser power) N_0 dependence of the PA, PL, and PLDMR signals is analyzed by means of a rate equation model, which describes the dynamics of singlet excitons (SE's) and polarons in all three experiments quantitatively with the same set of parameters. The model is based on the observations that mobile SE's are quenched by trapped and free polarons and that the spin-$\frac{1}{2}$ magnetic resonance conditions reduce the total polaron population. Since the sublinear N_0 dependences of the positive (PL-enhancing) spin-$\frac{1}{2}$ PLDMR and the polaron PA band are essentially the same, we conclude that PLDMR is due to a reduced quenching of SE's by polarons. The agreement between the model, the current results, and results from other spectroscopic techniques provides strong evidence for this quenching mechanism. This also suggests that it is a very significant process in luminescent π-conjugated materials and organic light-emitting devices. Consequently, the quenching mechanism needs to be taken into account, especially at high excitation densities, which is of great importance for the development of electrically pumped polymer laser diode structures.

DOI: 10.1103/PhysRevB.64.155204 PACS number(s): 71.38.−k, 72.80.Le, 78.20.Ls, 78.55.Kz

I. INTRODUCTION

The methyl-substituted poly(*para*-phenylene)-type ladder-polymer (*m*-LPPP) is highly attractive for applications in organic light-emitting diodes[1] (OLED's) and as the active medium in organic solid-state lasers[2] due to its high photoluminescence (PL) quantum yield $\eta_{PL} \sim 30\%$ in film and $\sim 100\%$ in solution,[3] and the high interchain order in the solid state.[4,5] From previous studies on *m*-LPPP a comprehensive picture of the generation of polarons[6–8] and triplet excitons[8,9] (TE's) from singlet excitons (SE's) was drawn. It is well known that polarons, as found in OLED's upon injection of carriers,[10] recombine to form SE's, which generate the electroluminescence (EL). However, to our knowledge there is no quantitative model which describes the interaction of SE's with polarons and TE's in this class of materials. It has only been suggested that mobile SE's (Ref. 11) are nonradiatively quenched by polarons,[12] similar to quenching by defects such as carbonyl groups.[13] In contrast to molecular crystals such as para-hexaphenyl,[14] conjugated polymers exhibit strong polaronic photoinduced absorption (PA) bands,[9,15] so there is a need to quantify the interaction of polarons and SE's. Moreover, single crystals of small π-conjugated molecules such as tetracene, which do not contain grain boundaries defects that stabilize polarons,[16] have very recently led to electrically pumped organic solid-state lasers.[17]

This work shows that a polaron density $n_p \sim 10^{17}\,\mathrm{cm}^{-3}$ will lead to a nonradiative quenching rate of SE's which is comparable to the radiative decay rate. The density due to injected carriers in OLED's ranges typically from $\sim 10^{12}\,\mathrm{cm}^{-3}$ at low driving current to $\sim 10^{18}\,\mathrm{cm}^{-3}$ under intense pulsed currents.[18] However, even at low currents polaron densities as high as $10^{17}\,\mathrm{cm}^{-3}$ can build up by trapping at defect sites, as found by thermally stimulated current[16,19] (TSC) and PA measurements.[19]

In order to probe the interaction of polarons with SE's, one needs to vary their density and simultaneously detect their effect on the SE's. PA-detected magnetic resonance (PADMR) measurements show that at the spin-$\frac{1}{2}$ field-for-resonance the polaron and TE populations decrease.[9,20] Therefore, PL-detected magnetic resonance (PLDMR), which typically includes a PL-enhancing (i.e., positive) spin-$\frac{1}{2}$ polaron resonance,[21] is an ideal tool to probe the influence of the decreasing polaron population on the SE's. However, two mechanisms have been suggested to account for this resonance: (a) polarons acting as quenching centers for SE's; hence a reduced polaron population leads to a reduced rate of SE quenching, and consequently an enhanced PL intensity (I_{PL}) (Ref. 21); and (b) magnetic resonance enhancement of the formation of TE's from geminate polaron pairs, followed by TE-TE annihilation to SE's, resulting in an enhanced PL due to delayed fluorescence.[22] However, as mentioned above, recent PADMR results have shown that as one reduces the population of polarons at the spin-$\frac{1}{2}$ field-for-resonance (i.e., at $g \approx 2.002$), one simultaneously observes a

decrease in the TE population.[9] Since an enhancement of the TE population is a key requirement for the observation of an enhancement in I_{PL} due to triplet-triplet annihilation, this second mechanism is ruled out.

Based on the fact that polarons quench SE's, in this paper we quantify the significance of this interaction by analyzing the cw excitation density dependence of I_{PL}, the PA, and PLDMR signals of *m*-LPPP and the seven-membered ladder-type oligo(*para*-phenylene) (LOPP7) with a rate equation model. The model, which will be derived, quantifies the ongoing photophysical processes of polarons as observed in PA and PADMR, of SE's as seen in PL, and the interaction between them as found in PLDMR. Comparison of the model with the excitation density N_0 dependences of I_{PL}, the polaron PA bands, and the spin-$\frac{1}{2}$ PLDMR amplitude suggests that quenching of SE's at polarons affects the efficiency of OLED's and is therefore relevant to the development of OLED's as well as electrically pumped organic solid-state lasers.

II. EXPERIMENTAL PROCEDURE

The synthesis of *m*-LPPP and LOPP7 (see inset of Fig. 1) is described elsewhere.[23,24] Samples were prepared for PLDMR measurements by dissolving the polymer or oligomer powder in toluene in a 4-mm-o.d. quartz tube. The toluene was then evaporated, leaving a ~200-nm-thick film on the inside walls of the tube. Solution samples were prepared by freezing the 3-mg/ml toluene solution in a quartz tube, degassing it, and vacuum sealing the tube. The sealed sample tubes were placed in the quartz Dewar of an Oxford Instruments He-gas-flow cryostat, enabling temperature control from 4 to 300 K, inside an optically accessible *X*-band microwave cavity (microwave frequency of 9.35 GHz). Two types of PLDMR spectra are presented: (i) the *H*-PLDMR spectrum, in which the normalized microwave-induced change in the spectrally integrated PL ($\Delta I_{PL}/I_{PL}$) emitted by the sample is measured, while sweeping the magnetic field *H*; (ii) the λ-PLDMR spectrum, in which the microwave-induced change in the PL (ΔI_{PL}) is measured at the peak of the resonance (i.e., at that constant magnetic field). The *H*-PLDMR spectra were measured using a Si photodiode. The PL was excited at 457.9 nm by a Pockels-cell-stabilized Ar^+ laser. The excitation power was kept at or below 50 mW to prevent sample heating. The laser line was blocked by an appropriate cutoff filter. The *X*-band microwave-induced change in I_{PL} was detected by feeding the photodiode output into a lock-in amplifier referenced to the microwave chopping frequency $89 \leqslant \nu_c \leqslant 10$ kHz. The microwave power was kept below 810 mW. No saturation effects for microwave powers up to 1.7 W have been observed. The λ-PLDMR spectra were recorded by replacing the photodiode by a monochromator and a photomultiplier tube. For the λ-PLDMR spectra ~10 mW UV excitation was provided by a 200-W xenon lamp in combination with appropriate mirrors and bandpass filters.

The film for PADMR measurements was prepared by dropcasting a toluene solution of *m*-LPPP. The sample was positioned in the He-gas-flow cryostat inside the optically accessible *X*-band microwave cavity. The PADMR is obtained by measuring the microwave-induced change (δT) in the transmission *T* through the film. As in PLDMR, two types of PADMR spectra are presented: (i) the *H*-PLDMR and (ii) the λ-PADMR spectra. (i) For the *H*-PLDMR spectrum, the normalized microwave-induced change in the transmission $\delta T/T$ through the sample at a certain wavelength position, typically at the peak of a PA band, is measured, while sweeping the magnetic field *H*. (ii) For the λ-PADMR spectrum the unnormalized microwave-induced change in the transmission, δT, is measured at a constant *H*, typically at the peak of the resonance. The transmitted light provided by a 100-W tungsten lamp was waveguided into the monochromator and detected by a Si photodiode. The sample was excited at 457.9 nm by an Ar^+ laser. The microwave-induced changes δT were detected by a lock-in amplifier as for PLDMR. For all PADMR measurements the microwaves were chopped at 89 Hz and all spectra were corrected for the optical throughput of the setup.

The samples for PA and measurements were prepared as for PADMR. The 457.9-nm pump beam was produced by an Ar^+ laser, which was mechanically chopped at 89 Hz providing the reference for the lock-in amplifier. For the measurements the sample was mounted in an optically accessible cryostat under a dynamic vacuum of less than 10^{-5} mbar to prevent photo-oxidation. Hence no significant sample degradation was observed during measuring time periods exceeding 100 h. A 200-W halogen lamp provided the light source for the transmission measurement. All PA spectra were measured at 77 K and were corrected for the PL and optical throughput of the setup.

The number of photons incident on a unit cross-sectional area of the sample per second is

$$N_0 = P/(h\nu A), \tag{1}$$

where *P* is the laser power, $h\nu$ the photon energy, *A* the cross-sectional area of the laser beam, and *d* the thickness of the sample. Within the sample the number of absorbed photons follows Beer's law so that the average density of SE's generated per second is

$$n_{SE} = (N_0/d)[1 - \exp(-\alpha d)], \tag{2}$$

with α the absorption coefficient. To account for their modulation frequency ν_c dependence, the PLDMR,[25] PA, and PADMR data were recorded at frequencies low enough compared to the lifetimes of the involved recombination processes, i.e., $\nu_c \tau \leqslant 1$, in order to ensure that the steady-state solutions as used to model the data are valid. This has been tested by measuring the N_0 dependence of the total polaron population in PA for frequencies up to 1700 Hz. For frequencies $\nu_c < 100$ Hz we did not observe any qualitative differences in the N_0 dependence. We did see a decrease in the overall intensity of the signal, which was corrected by extrapolating to $\nu_c = 0$.

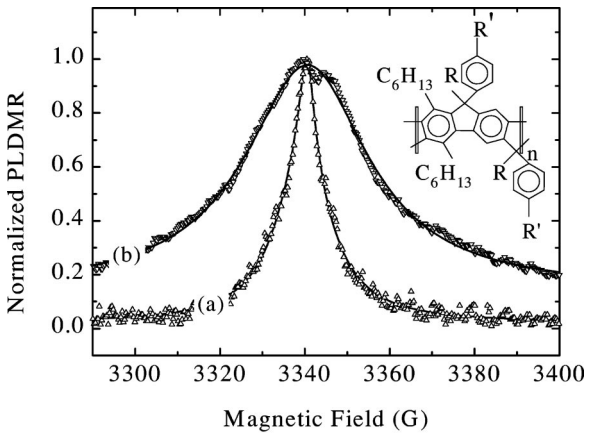

FIG. 1. Polaron resonances of (a) pristine *m*-LPPP film and (b) LOPP7 film at $T=20\,\mathrm{K}$, $\lambda_{exc}=457.9\,\mathrm{nm}$, and microwave power 810 mW. The lines are the Lorentzian fits to the observed spectra. The inset shows the chemical structure of the ladder-type poly(*p*-phenylene); for *m*-LPPP, $R=CH_3$, $R'=C_{10}H_{21}$, $n\approx 12$; for LOPP7, $R=H$, $R'=C_4H_9$, and the conjugated backbone consists of seven phenyl rings.

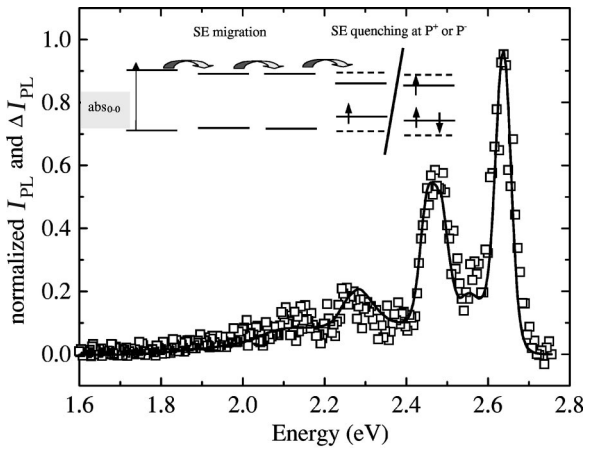

FIG. 2. λ-PLDMR and PL spectrum of an *m*-LPPP film recorded at 20 K. The symbols show ΔI_{PL}, the lines I_{PL}. The inset shows a schematic drawing of the quenching of a migrating SE at a polaron.

III. EXPERIMENTAL RESULTS

Figure 1 shows the polaron H-PLDMR at $g=2.002$ of (a) an *m*-LPPP film and (b) an LOPP7 film. Its full width at half maximum $\Delta H_{1/2}$ is (a) 11 G and (b) 40 G, respectively. This difference in $\Delta H_{1/2}$ is attributed to the decreased polaron pair separation (and hence increasing dipolar broadening) in the oligomer, in agreement with results found from a comparison of these resonances in frozen *m*-LPPP solutions and *m*-LPPP films.[25,26] There it was found that $\Delta H_{1/2}$ is drastically reduced in solution due to the increased chain separation. In the polymer and oligomer of this work the situation is similar due to the much smaller side groups of the latter. Both materials have C_6H_{13} groups to provide solubility, but the additional long $C_{10}H_{21}$ side groups of the polymer, which are efficient spacers between the molecules in the film, are replaced by CH_3 groups in the oligomers. Hence adjacent oligomer chains are much closer than the polymer chains, which reduces the average separation of interchain polaron pairs and consequently broadens the PLDMR spectrum.

Figure 2 shows that the PL and ΔI_{PL} spectra of an *m*-LPPP film at 20 K are essentially identical. They exhibit a 0-0 transition from the lowest unoccupied molecular orbital (LUMO) to the highest occupied molecular orbital (HOMO) at 2.69 eV and two well-resolved vibronic replica spaced 180 meV apart. Due to the much lower signal-to-noise ratio of the resonance in LOPP7, no clear ΔI_{PL} spectrum of that film could be obtained. The inset shows a schematic drawing of the SE-polaron interaction as discussed below.

Figure 3 shows that the amplitude $\Delta I_{\mathrm{PL}}/I_{\mathrm{PL}}$ of the polaron resonance in both *m*-LPPP and LOPP7 films increases with N_0. Fitting the dependence to a power law

$$\Delta I_{\mathrm{PL}}/I_{\mathrm{PL}}=aN_0^b, \tag{3}$$

one finds $b=0.79$ for $N_0<5\times10^{21}\,\mathrm{photons\,cm^{-3}\,s^{-1}}$ and $b=0.56$ for higher N_0. For LOPP7, $b=0.55$ over the measured range. For clarity in the plot we do not show the lines for the power-law fit, but only the results of the fit to the model as derived below. We note that I_{PL} of both *m*-LPPP and LOPP7 was directly proportional to the laser power over the measured range.

The top graph in Fig. 4 shows the PA spectrum of an *m*-LPPP film. It exhibits two distinct features, the triplet-triplet transition $T_1\rightarrow T_n$ at 1.3 eV and the polaron $P2_{0\text{-}0}$ band at ~1.9 eV. The ~2.1-eV ($P2_{0\text{-}1}$) band is a vibronic replica of the ~1.9-eV band. These assignments were deduced from a comparison of the PA with doping- and charge-induced absorption spectra, which only yielded the 1.9–2.1 eV bands.[10] The bottom spectrum shows the λ-PADMR spectrum of an *m*-LPPP film recorded at the peak of the spin-$\frac{1}{2}$ resonance. The spectrum clearly shows that the absorption feature of the triplet exciton at 1.3 eV and that of the polaron at 1.9 and 2.1 eV are both reduced at the field for the spin-$\frac{1}{2}$ resonance as observed for measurements taken in an *S*-band microwave cavity.[9] As expected, for the same microwave power,[27] the magnetic resonance-induced drop in the polaron population, as measured by $\delta T/\Delta T$ of the polaron

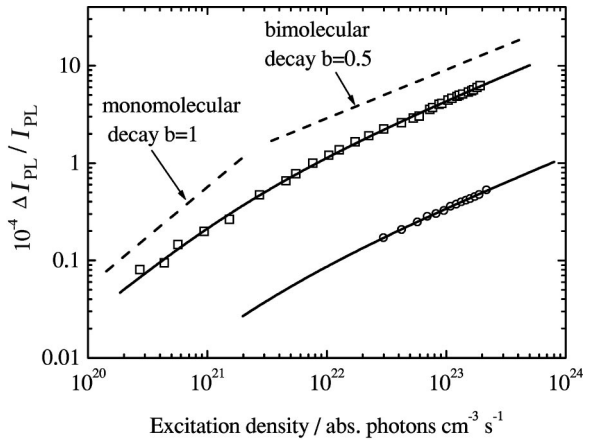

FIG. 3. Excitation density dependence of PLDMR at $g=2$ of (a) *m*-LPPP and (b) LOPP7 recorded at the peak of the resonances shown in Fig. 1. The solid lines represent a fit to Eq. (17).

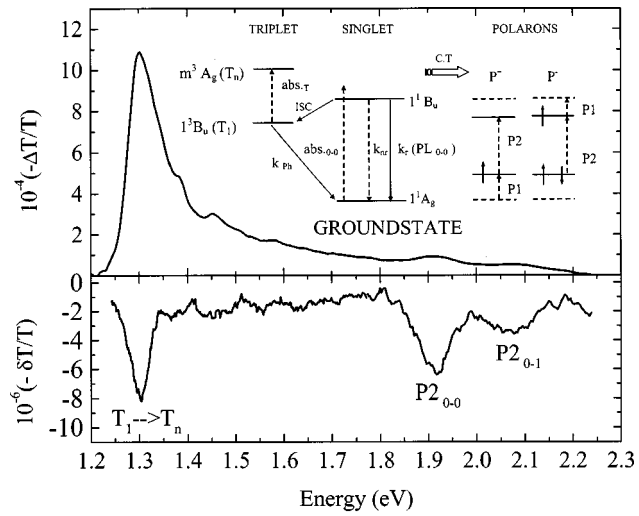

FIG. 4. Top: photoinduced absorption (PA) spectrum of an *m*-LPPP film recorded at 80 K with an excitation density of 2×10^{22} photons $cm^{-3}\,s^{-1}$. Bottom: photoinduced absorption detected magnetic resonance spectrum (PADMR) of an *m*-LPPP film recorded at 20 K with an excitation density of 5×10^{22} photons $cm^{-3}\,s^{-1}$. Inset top: the energy levels and optical transitions associated with singlet, triplet, and charged excitations. The $1A_g$ and the $1\ ^3B_u$ states are the ground state and lowest TE states, respectively. The $1\ ^1B_u$ is the lowest allowed excited SE state. k_r and k_{nr} are the radiative and nonradiative rate constants of the $1\ ^1B_u$ SE, "abs$_T$" denotes the triplet absorption from the $1\ ^3B_u$ to the lowest excited state m^3A_g, while k_{PH} is the radiative phosphorescent decay of triplets to the ground state. p^+ and p^- represent polarons created upon charge transfer (CT), while $P1$ and $P2$ are the observed optical transitions between polaron states in photoinduced absorption.

band at 1.9 eV, is much stronger at the *X* band, where it is approximately 6%, than at the *S* band, where it was found to be about 3% at a similar microwave power.

Figure 5 shows the PADMR amplitude $\delta T/T$ of the $P2$ band of *m*-LPPP as a function of N_0 on a log-log scale. $\delta T/T$ exhibits a power-law dependence similar to that of the polaron PLDMR $\Delta I_{\mathrm{PL}}/I_{\mathrm{PL}}$:

$$\delta T/T = aN_0^b, \tag{4}$$

with $b\cong0.57$ over the entire measured range. The inset shows the *H*-PADMR polaron resonances with the transmission set to 1.9 eV. The fit to a single Lorentzian line yields $\Delta H_{1/2}\approx12$ G. The fact that $\Delta H_{1/2}$ is effectively the same as that of the PLDMR demonstrates that the same polaron pairs are probed in both measurements.

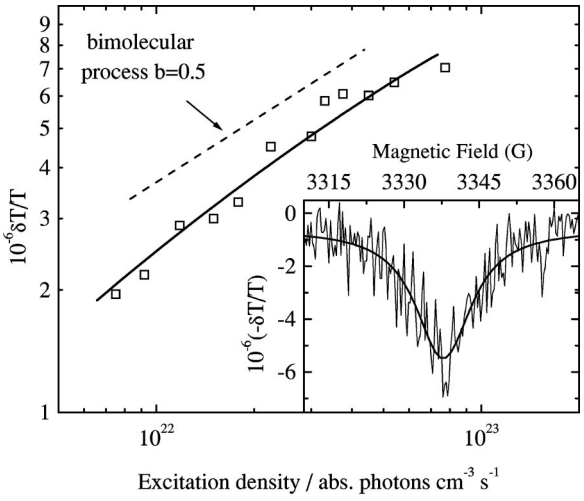

FIG. 5. Excitation density dependence of the polaron PADMR feature at 1.9 eV of an *m*-LPPP film recorded at the peak of the $g=2$ resonance. The line is a guide to the eye. Inset: *H*-PADMR polaron resonances at $g=2$ recorded for the polaron feature at 1.9 eV ($\lambda=653$ nm).

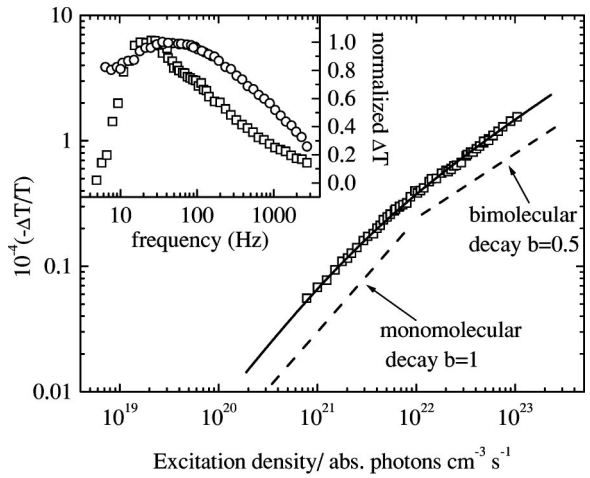

FIG. 6. Excitation density dependence of the polaron PA feature at 1.9 eV of an *m*-LPPP film. The line is the fit of Eq. (13). Inset: the quadrature component of the lock-in signal as a function of the chopping frequency ν_c, recorded at an excitation density of 10^{21} photons $cm^{-3}\,s^{-1}$ (circles) and 5×10^{22} photons $cm^{-3}\,s^{-1}$ (squares).

The inset in Fig. 6 shows the dependence of the quadrature signals of the lock-in amplifier on υ_c at $N_0=10^{21}$ and 6×10^{22} photons $cm^{-3}\,s^{-1}$. As described in detail in Refs. 9 and 22, if $\nu_{c,\max}$ is the frequency at which the quadrature signal is at its maximum, then the polaron decay rate is

$$2k_p = 2/\tau_p = 2\pi\nu_{c,\max}, \tag{6}$$

where τ_p is the polaron lifetime. This relation yields $k_p=63\ s^{-1}$ and $\tau_p=15.8$ ms at the lower excitation density. The factor of 2 is due to the fact that each polaron recombination event removes two polarons from the system. At the higher

Figure 6 shows the intensity $\Delta T/T$ of the $P2$ band of *m*-LPPP as a function of N_0 on a log-log scale. In order to account for the underlying triplet-to-triplet ($T_1\rightarrow T_n$) transition, each point was corrected for that contribution at 2.0 eV. Here $\Delta T/T$ exhibits a power-law dependence similar to that of the polaron PLDMR $\Delta I_{\mathrm{PL}}/I_{\mathrm{PL}}$ and PADMR $\delta T/T$:

$$\Delta T/T = aN_0^b, \tag{5}$$

with $b=0.80$ and 0.57 for $N_0<5\times10^{21}$ photons $cm^{-3}\,s^{-1}$ and higher, respectively (the results of this fitting are not shown for clarity in the plot). The polaron PA band in LOPP7 exhibits a power-law dependence with $b=0.49$,[28] which is also similar to $\Delta I_{\mathrm{PL}}/I_{\mathrm{PL}}$ in that oligomer.

N_0 the ν_c dependence of the quadrature signal exhibits a much broader maximum slightly shifted towards higher frequencies and a much weaker roll-off at higher frequencies, due to the faster decay dynamics of the contribution of a bimolecular recombination kinetics. A detailed analysis and discussion of this signal and of the peak position can be found below in Sec. IV D.

IV. ANALYSIS AND DISCUSSION

To study the nature of the interaction between polarons and SE's as observed in the PLDMR and PL and the dynamics of polarons as observed in the PA on a quantitative basis, a rate equation model is derived and discussed. The obtained equations are then used to model the excitation dependences of I_{PL}, the PA, and the PL-enhancing polaron PLDMR. The obtained results are discussed in relation to results from other spectroscopic techniques such as TSC and PADMR, and general conclusions for the operation of polymer light-emitting diodes and possible future laser diode applications are drawn.

A. Singlet-exciton dynamics

SE's are the primary photoexcitations in conjugated polymers. They are created by an absorbed photon promoting an electron from the HOMO to the LUMO, yielding a bound electron-hole pair. Following their creation and prior to their radiative or nonradiative decay or dissociation, they are subject to migration driven by the energetic disorder in the conjugated polymer, which is manifest in the inhomogeneous broadening of the optical spectra.[29] This is a consequence of the small local variations in the overlap of π electrons and hence the energy difference between the HOMO and LUMO.[30,31]

The excitation energy migration can be described as a combination of one-dimensional (1D) on-chain migration as well as 3D Förster transfer.[32] We therefore assume a quasi-3D migration of SE's in a 3D isotropic medium. However, the good agreement between our data and our model justifies the simplifications required to describe these types of measurements with this class of materials. In fact, we have recently found that if the polymers' chains are isolated in a matrix ordered at the nanometer scale, in which 3D SE migration is inhibited, the PL and PLDMR are markedly different from the bulk polymer.[33]

As demonstrated for poly(*para*-phenylene vinylene) (PPV) (Ref. 13) and *m*-LPPP (Refs. 26 and 34), photooxidation of the material strongly quenches the PL. This was attributed to induced defects, such as carbonyl groups, acting as quenching sites for migrating SE's. Yet a similar nonradiative quenching process should occur if a SE S_1^* encounters a trapped or free polaron $p^{+/-}$:

$$p^{+/-} + S_1^* = S_0 + \text{phonons} + p^{+/-}, \tag{7}$$

where S_0 is the singlet ground state. We note that a similar process was found in crystals of small organic molecules.[35] However, there is a fundamental difference between quenching at chemical defects such as carbonyl groups and quenching by polarons: the density of chemical defects is independent of the excitation density, whereas the steady-state polaron density increases with increasing excitation density since polarons are generated from SE's.[9] Hence the rate equation for the dynamics of the SE's including radiative and nonradiative processes is given by

$$\frac{dn_{\mathrm{SE}}}{dt} = N_0 - (k_r + k_{nr} + \gamma_q n_P) n_{\mathrm{SE}}, \tag{8}$$

where n_p is the total density of polarons, and k_r and k_{nr} are the radiative and nonradiative SE decay constants, respectively. k_{nr} includes nonradiative recombination via production of phonons as well as the creation of polarons, i.e., exciton dissociation. The polaron-SE annihilation rate constant γ_q is a measure of the interaction of the two quasiparticles. It accounts for mobile SE's getting quenched at trapped immobile polarons and for trapped SE's getting quenched by diffusing polarons (also see below).

From the steady-state solution of Eq. (8), one finds the dependence of I_{PL} on N_0:

$$I_{\mathrm{PL}} \propto n_{\mathrm{SE}} k_r = \frac{k_r N_0}{k_r + k_{nr} + \gamma_q n_p}. \tag{9}$$

As easily seen, the nonradiative quenching rate of SE's by polarons, $\gamma_q n_p$, is a function of the mobility of polarons and SE's as well as the steady-state polaron and SE densities.

B. Polaron dynamics in PA

Upon photoexcitation, an equal density of positive n_{p+} and negative n_{p-} polarons is created by dissociation of SE's, yielding a total polaron density

$$n_p = n_{p+} + n_{p-}. \tag{10}$$

The dissociation, i.e., the creation yield of polarons, is enhanced by an external electric field,[7] by chemical defects,[26] and by energetic disorder of the material. In addition, n_p also depends on the polaron lifetime τ_p. As depicted in the inset of Fig. 4, in principle two different polaron absorption features can be found in the PA spectrum. The $P1$ and $P2$ bands are usually located in the near-infrared (NIR) and visible regions of the spectrum, respectively. For both bands there are two different regimes of polaron recombination: the monomolecular, as found at low N_0 or in isolated systems, and the bimolecular, observed at high N_0.

1. Monomolecular regime

At low N_0 as well as in systems where the polymer chains are isolated, such as in solution,[36] one finds a predominantly linear dependence of the polaron population, as manifest in the polaron PA bands, on N_0, reflecting monomolecular decay dynamics. Since polarons can only recombine mutually, the linear regime is due to geminate polaron recombination. This must result from ''incomplete'' exciton dissociation, without subsequent creation of free polarons. Hence the two polarons which recombine mutually form a geminate polaron pair during their lifetime. Such pairs can be formed by a

charge transfer process between two conjugated chain segments on the same chain, resulting in intrachain interconjugation segment pairs or interchain pairs, with the polarons located on adjacent segments of different chains. Since such pairs are very unstable due to the Coulomb attraction of the two oppositely charged polarons, a potential barrier is required to prevent immediate recombination. In the case of an intrachain interconjugation pair, such a barrier can be provided by an impurity or a static or dynamic structural defect in the polymer backbone. For interchain pairs the initial gain in energy, driving the charge transfer process, will be sufficient as an energetic barrier to prevent immediate back transfer and recombination of the pair. The geminate recombination rate of polarons is described by the rate equation

$$\frac{dn_p}{dt} = \eta_p N_{\mathrm{SE}} - 2k_p n_p , \tag{11}$$

with k_p the decay constant of geminate polaron pairs and $\eta_p N_{\mathrm{SE}}$ the formation rate of polarons from SE's with $N_{\mathrm{SE}} = n_{\mathrm{SE}}(k_{nr} + \gamma_q n_p)$ and n_{SE} from the solution of Eq. (8). The factor of 2 in Eq. (11) is due to the fact that each recombination event reduces the number of polarons by 2.

2. Bimolecular decay

The bimolecular decay dynamics found at high N_0 is due to nongeminate recombination of ''free'' polarons, i.e., polarons which were completely separated from the oppositely charged polaron with which they were created. Such ''free'' polarons, however, are trapped either at a defect or at a local energy minimum within the energetically disordered density of states.

For *m*-LPPP, TSC measurements have revealed mostly shallow traps with a density of at least $2\times10^{16}\,\mathrm{cm}^{-3}$ for polarons with an average activation energy of 60 meV,[26] in agreement with the energetic disorder parameter $\sigma = 50\,\mathrm{meV}$ (Ref. 37) found from time-of-flight measurements. Therefore, at the measurement temperature of 77 K hardly any thermal detrapping of polarons can be expected, which is confirmed by the fact that the TSC was found to be independent of the delay between the creation of the polarons at low temperatures and the detection of the current upon heating.

At low temperature where no thermal detrapping can be found, there is still, however, a bimolecular term due to mobile polarons (which are not yet trapped) which recombine with other polarons—either trapped or also mobile. Such a process yields a bimolecular term at any temperature. Yet as the temperature is increased one finds that in addition to this process detrapping enhances the bimolecular recombination term, which speeds up the recombination and reduces the overall steady-state density of polarons, as verified by experiments.[8] Moreover, we have observed a clear photovoltaic response at temperatures as low as 20 K, which demonstrates that polarons maintain a certain mobility to yield a bimolecular recombination even at such low temperatures.

The bimolecular recombination process of polarons is described by the term $-\gamma_p n_p^2$ in the rate equation for the polaron population. The bimolecular annihilation rate constant γ_p is a measure of the polaron diffusivity and combines the contributions from trapping and detrapping processes. The former are due to thermal activation processes at higher temperatures and the latter to the interaction with light or other entities such as SE's or TE's. In this context it is worth noting that in molecular crystals it has been found that the interaction of a TE with a geminate polaron pair increases the recombination probability of the polaron pair.[35] Such a process is also feasible for the encounter of a polaron pair with a SE in the present materials. Since such an interaction process between two entities depends on the density of the two entities and the interaction strength, it leads to the observation of a sublinear dependence of the polaron population on N_0. However, as modeling of such processes with rate equations shows, one only finds a general sublinear dependence for such a process and not an explicit bimolecular dependence of the polaron population on N_0, as observed in this study. Therefore, we did not include such processes in our model and we conclude that in order to describe the polaron excitation dependence over a wide range of N_0 one needs to combine the contribution from the monomolecular geminate recombination [Eq. (11)] and the bimolecular nongeminate decay term into one equation, which yields

$$\frac{dn_p}{dt} = \eta_p N_{\mathrm{SE}} - 2k_p n_p - \gamma_p n_p^2 \tag{12}$$

and its steady-state solution

$$n_p = \frac{-k_p + \sqrt{k_p^2 + \eta_p \gamma_p N_{\mathrm{SE}}}}{\gamma_p}. \tag{13}$$

For a simple comparison with PA, Eq. (13) can be approximated by the power-law dependence $n_p \approx a N_0^b$, with $0.5 \leqslant b \leqslant 1$, given by Eq. (5). The value of b depends on whether monomolecular or bimolecular recombination dominates, as manifest in the different slopes seen in Fig. 6. Yet to relate the intensity of the PA to the steady-state density of polarons in the sample the following must be considered: The PA measurement probes the photoinduced change in transmission $\Delta T/T$, which is proportional to the density of the probed excitations, n. With the absorption cross section σ and the film thickness d, the relation $n_p = -\ln(1 - \Delta T/T)/(\sigma d) \approx (\Delta T/T)/(\sigma d)$, valid since $\Delta T/T \ll 1$, yields

$$n = (\Delta T/T)/(\sigma d). \tag{14}$$

Semiempirical Hartree-Fock intermediate neglect of differential overlap (INDO) and configuration interaction (CI) quantum chemical calculations indicate that the absorption cross sections of the singlet ground state, polarons, and low-lying triplets are all comparable.[38] Doping-induced absorption measurements on *m*-LPPP led to similar conclusions on the polaron absorption.[39] Given the absorption coefficient $\alpha \sim 10^5\,\mathrm{cm}^{-1}$ for *m*-LPPP, one finds the effective singlet absorption cross section for a randomly oriented bulk polymer from $\sigma = \alpha/N$, with N the density of ground states. Assuming $N = \rho N_A / m_W$,[40] where ρ is the density, N_A is Avogadro's number, and m_W is the molecular weight of the repeat unit, we get $\sigma = m_W \alpha / \rho N_A$. From $m_W \sim 800$ and $\rho = 0.6\,\mathrm{g/cm}^3$ (Ref. 41) one finds $\sigma_{\mathrm{SE}} \sim 2\times10^{-16}\,\mathrm{cm}^2$.

C. Magnetic resonance experiments

As shown in Fig. 4, PADMR measurements show that the spin-$\frac{1}{2}$ resonance conditions at $g \approx 2.002$ decrease the polaron and TE populations.[9] In contrast to an electron spin resonance (ESR) experiment, which probes the absorption of microwaves by the polarons, a reduction of the polaron population requires an enhancement of the mutual spin-dependent recombination of geminate and/or nongeminate polaron pairs. If the polaron spin-lattice relaxation time $T_1 \ll \tau_p$, then that recombination becomes effectively spin independent. Hence the observation of a PLDMR suggests that $T_1 > \tau_p$. Unfortunately, the authors are unaware of measurements of the polaron T_1 in any π-conjugated polymer. Hence, assuming that $T_1 > \tau_p$, one can describe the effect of resonant microwaves at the field for resonance. The kinetics of polarons and polaron pairs can be treated as a quasistationary spin-level system by a set of coupled kinetic rate equations.[42] A rather comprehensive recombination scheme for geminate polaron pairs has been described by Dyakonov *et al.* assuming $T_1 \sim 10^{-7}$ s and a geminate polaron pair lifetime of $\sim 10^{-7}$ s as well.[22] This scheme, however, cannot be applied to the present study since the PA measurements indicate that in *m*-LPPP films the overall polaron lifetimes are from 100 μs to 10 ms. Moreover, the geminate polaron pair model cannot account for the PADMR results shown in Fig. 4 (see also Ref. 9 for measurements at the *S* band), since it predicts an enhancement of the interchain TE population from geminate polarons, whereas a decrease in the population was observed at the spin-$\frac{1}{2}$ field for resonance.

In order to discuss the conditions required to observe a PLDMR due to recombination of nongeminate polaron pairs, let us compare PLDMR to EL-detected magnetic resonance (ELDMR). It is reasonable to assume that the effect of magnetic resonance conditions on the nongeminate polaron pairs is the same in PLDMR, where polarons are formed from dissociating SE's, as in ELDMR where polarons are formed from injected charges. Previous ELDMR measurements on *m*-LPPP have yielded strong resonances of order $\Delta I_{\mathrm{EL}}/I_{\mathrm{EL}} \sim 10^{-3}$.[43] These results demonstrate that one can strongly alter the recombination yield of nongeminate pairs at the field for resonance, since carrier injection generates no geminate pairs. Moreover, the N_0 dependence of the PADMR of the polaron $P2$ band at the spin-$\frac{1}{2}$ field for resonance shown in Fig. 5 is strongly sublinear ($\propto I^{0.57}$), providing a clear indication of enhancement of bimolecular nongeminate polaron recombination. From these experimental results we conclude that nongeminate recombination of polarons is enhanced at the spin-$\frac{1}{2}$ field for resonance.

To explain the magnetic resonance enhancement of nongeminate recombination of polarons, we propose the following model. We note, however, that further investigations, especially the determination of T_1, will be required in order to describe the nongeminate recombination on a quantitative basis.

Following their generation by complete SE dissociation, the unpaired polarons are an uncorrelated spin-$\frac{1}{2}$ system, which will relax to the Boltzmann distribution in time T_1. Since quantum chemical calculations for oligophenyls[44] show that polarons which are separated by a distance of one phenyl ring can already by treated as uncorrelated, we assume that the magnetic resonance enhancement of both nongeminate and geminate recombination works in a similar way. In order to recombine, the polarons must form a correlated pair, with sufficient spin polarization so that at the field for resonance one can sufficiently enhance the recombination of the pairs and, hence, decrease the total polaron population.

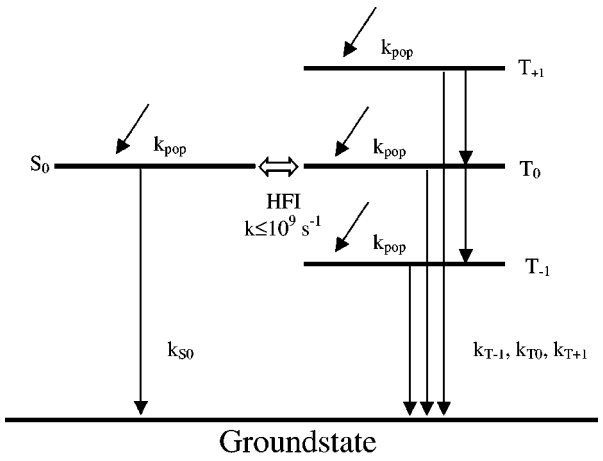

FIG. 7. Schematics for nongeminate polaron recombination at the field for resonance (for explanation, see text).

As shown in Fig. 7, spin statistics mandate that upon random encounter, two spin-$\frac{1}{2}$ polarons will form triplet and singlet polaron pairs with a ratio 3:1 and populate the four magnetic sublevels with the same rate constants k_{pop}. As shown in Fig. 7, the S_0 and T_0 states of polaron pairs are degenerate and the hyperfine interaction process mixes the population of these magnetic sublevels[42] with a rate up to $10^9\ \mathrm{s}^{-1}$ as explained in detail in Ref. 42 and references therein.

The singlet pairs will decay radiatively (if they yield a SE) or nonradiatively to the singlet ground state. The triplet pairs will decay to TE's. Yet recent experimental and theoretical studies[45] suggest that in PPV LED's the ratio of TE's to SE's resulting from nongeminate polaron recombination is less than 3:1 and may be as low as 1:1. This suggests that the decay rates of the T_{-1}, T_0, and T_{+1} triplet pair states to TE's is less than that of the S_0 singlet pair state to SE's, i.e., k_{T-1}, k_{T0}, and $k_{T+1} < k_{S0}$. Such a situation will result in polarization of the spin states of the polaron pairs in the T_{-1}, T_0, and T_{+1} levels, which will have a higher steady-state density than the S_0 state of polaron pairs, as the observation of the PLDMR and PADMR requires that the spin-lattice relaxation time T_1 be longer than the time the two polarons form a pair. Hence the polaron recombination rate is not determined by the lifetime of the pairs, but by the rate at which a polaron encounters another polaron, which in turn is determined by the polaron mobility.

In short, at steady state one finds a situation in which S_0 is less populated than T_{-1}, T_0, or T_{+1}. Absorption of microwaves at resonance induces a net population transition from T_{-1}, T_0, and T_{+1} to S_0 and thereby enhances the recombination of the overall polaron pair population. Hence this proposed reaction kinetics for polaron pairs can account for the

TABLE I. Parameter values used to fit the PL and PLDMR excitation density dependence of Fig. 3 with Eqs. (9) and (17). For explanation of the symbols see text.

Sample	k_r (s^{-1})	k_{nr} (s^{-1})	k_p (s^{-1})	γ_p ($cm^3 s^{-1}$)	γ_q ($cm^3 s^{-1}$)	η_p	$\Delta\gamma_q$ ($cm^3 s^{-1}$)	Δk_p (s^{-1})	$\Delta n_P/n_P$ (%)
m-LPPP	1×10^9	1×10^9	63	1.1×10^{-14}	0.9×10^{-9}	8×10^{-4}	7×10^{-16}	2	−4
LOPP7	2×10^9	4×10^{10}	63	1.1×10^{-14}	0.9×10^{-9}	8×10^{-4}	5×10^{-16}	1	−3

magnetic resonance-induced reduction in the overall polaron and TE population, as shown by PADMR, which recently has been used to determine the SE and TE formation cross section for photogenerated polarons.[46]

The total change in the recombination of polarons under spin-$\frac{1}{2}$ resonance conditions is therefore a result of the enhancement of the geminate and nongeminate decay rate constants k_p and $\gamma_p n_p$, respectively:

$$\frac{\Delta n_p}{n_p}=\frac{1}{n_p}\frac{dn_p}{dk_p}\Delta k_p+\frac{1}{n_p}\frac{dn_p}{d\gamma_p}\Delta\gamma_p, \tag{15}$$

with $\Delta\gamma_p$ and Δk_g the magnetic resonance-induced changes in k_p and γ_p, respectively. The PADMR shows that the total change $\Delta n_p/n_p$ is up to a few percent (see Sec. III above).

The PLDMR experiment probes the change in the steady state I_{PL} at the field-for-resonance. Since polarons act as quenching sites for SE's, a reduction in the polaron density induced by magnetic resonance conditions enhances I_{PL}.[21] We note that TE's can also act as SE quenching sites.[35] However, the contribution of a process in which a reduction of TE's leads to an enhanced PL can be neglected since TE's in general have a different signature in the *H*-PLDMR spectrum. As a consequence of the high localization of the TE's,[26] the interaction between the electron and hole causes a zero-field splitting (ZFS) of the different spin (sublevel) states of the TE. As a result of the ZFS, the resonance transitions for TE's are found at *g* values higher and lower than $g=2$. This is confirmed by PADMR where one finds a small change ($\Delta n/n<0.7\%$) in the TE density at the resonance position at $g=2$ (see Fig. 4).

In order to obtain a rate equation describing the excitation density dependence of the observed spin-$\frac{1}{2}$ PLDMR, one needs to substitute Eq. (13) into Eq. (9) and solve

$$\frac{\Delta I_{\mathrm{PL}}}{I_{\mathrm{PL}}}=\frac{1}{I_{\mathrm{PL}}}\frac{dI_{\mathrm{PL}}}{dk_p}\Delta k_p+\frac{1}{I_{\mathrm{PL}}}\frac{dI_{\mathrm{PL}}}{d\gamma_p}\Delta\gamma_p, \tag{16}$$

which yields the equation for the PLDMR with $\Delta\gamma_q$ and Δk_p the magnet-resonance-induced changes in the annihilation parameter γ_q and the decay constant k_p, respectively. The coupling between the variables of the equation leads to rather complex analytical expressions, which are not given here. However, as verified by numerical simulation, one finds that as long as the PL exhibits an almost linear increase with excitation density (i.e., $I_{\mathrm{PL}}\propto N_0^a$ with $a>0.95$), one can decouple Eq. (13) from Eq. (9) by substituting $\eta_{\mathrm{PL}}\eta_p N_0$ for $\eta_p N_{\mathrm{SE}}$, with η_{PL} the PL quantum yield. This leads to the final expression

$$\begin{aligned}\frac{\Delta I_{\mathrm{PL}}}{I_{\mathrm{PL}}}&=\frac{1}{I_{\mathrm{PL}}}\frac{dI_{\mathrm{PL}}}{dk_p}\Delta k_p+\frac{1}{I_{\mathrm{PL}}}\frac{dI_{\mathrm{PL}}}{d\gamma_p}\Delta\gamma_p\\&=\frac{(-k_p+R)\Delta k_p+\left(\dfrac{k_p^2-k_pR}{\gamma_p}+\dfrac{1}{2}\eta_{\mathrm{PL}}\eta_p N_0\right)\Delta\gamma_p}{\left(\dfrac{\gamma_p k_r+\gamma_p k_{nr}}{\gamma_p}-k_p+R\right)R},\end{aligned} \tag{17}$$

where

$$R\equiv\sqrt{k_p^2+\gamma_p\eta_{\mathrm{PL}}\eta_p N_0}. \tag{18}$$

D. Modeling of the PA, PL, and PLDMR

In order to model the excitation density N_0 dependence of the PLDMR of *m*-LPPP and LOPP7 shown in Fig. 3 using Eq. (17), we first consider the PA and I_{PL} results obtained for *m*-LPPP. This will reduce the set of adjustable parameters. All of the parameters appearing in Eq. (17) are listed in Table I.

1. Results obtained for m-LPPP

The radiative decay constant $k_r=10^9\,s^{-1}$ of *m*-LPPP is obtained from PL modulation spectroscopy. The absolute η_{PL} of *m*-LPPP films at room temperature is 30%. However, lowering the temperature to 20 K increases η_{PL} to 50% due to a lower nonradiative decay rate.[47] Since the intrinsic lifetime and, hence, k_r are determined by the quantum-mechanical transition matrix element, which is *per se* temperature independent, $k_{nr}=10^9\,s^{-1}$.

The excitation density dependence of the polaron $P2$ PA band at 1.9 eV is modeled by Eq. (13); here, $d=130$ nm, $\sigma_{\mathrm{polaron}}=2\times10^{-16}\,cm^2$, and $k_p=126/2=63\,s^{-1}$, as obtained from the ν_c dependence of the $P2$ band [see inset of Fig. 4; the factor of 2 is due to Eq. (5)]. Equation (13) then yields a polaron mutual annihilation parameter $\gamma_p=1.0\times10^{-14}\,cm^3\,s^{-1}$ and a polaron quantum yield (from SE dissociation) $\eta_p=8\times10^{-4}$. Furthermore, the mutual annihilation parameter γ_p can also be estimated from the maximum of the ν_c dependence in the inset of Fig. 6. Recent numerical simulations have shown[48] that one can also use the position of the maximum of the quadrature signal to estimate a equivalent decay constant k_{eq} since $2\pi\nu_{c,\max}\approx k_{\mathrm{eq}}$. From k_{eq} one can calculate γ_p from $k_{\mathrm{eq}}=\gamma_p N_{\mathrm{stst}}$, where N_{stst} is the steady-state concentration of polarons at the actual excitation density. For an excitation density of 5×10^{22} photons $cm^{-3}\,s^{-1}$, one finds $N_{\mathrm{stst}}=3.8\times10^{16}\,cm^{-3}$ and with

$\nu_{c,\max}=75$ Hz this yields $\gamma_p=1.2\times10^{-14}\,\mathrm{cm^3\,s^{-1}}$, which is in very good agreement with the value obtained from the fit of the excitation density dependence. With these values of k_p, γ_p, k_r, and k_{nr}, we now fit Eq. (17) to the spin-$\frac{1}{2}$ PLDMR excitation density dependence. For the fit, the total magnetic-resonance-induced change in the polaron density is set to $|\Delta n_p/n_p|\leqslant 0.06$, as determined from the PADMR of *m*-LPPP (see Sec. III above and Fig. 4). The obtained parameters are listed in Table I.

2. Results obtained for LOPP7

For LOPP7 the radiative decay constant $k_r=2\times10^9\,\mathrm{s^{-1}}$ is obtained from the PL decay dynamics. However, due to the much lower PL quantum yield $\eta_{\mathrm{PL}}\sim2\%$ in the solid state and assuming that its temperature dependence is similar to that of *m*-LPPP, one finds $k_{nr}=4\times10^{10}\,\mathrm{s^{-1}}$. For modeling the PLDMR excitation dependence, the same values for the parameters k_p and γ_p were used as obtained from the PA of *m*-LPPP. The resulting values of the parameters are also listed in Table I.

A first critical test for these values occurs in calculating the excitation dependence of I_{PL} from Eq. (9). We find that the parameters yield a nearly linear dependence ($I_{\mathrm{PL}}\propto N_0^{0.99}$), which is therefore in very good agreement with the linear behavior observed for both materials.

In order to evaluate the significance of the values of γ_p and γ_q obtained by fitting the model to the experimental results, we compare them with results from other spectroscopic techniques. The polaron annihilation rate constant γ_p, which is a measure of the polaron-polaron interaction, can be related to a diffusion coefficient $D=\gamma_p/4\pi R$, where $R=1$ nm is the extent of the polaron wave function, as found from quantum-chemical calculations.[49] The polaron mobility μ is then given by the Einstein relation

$$eD=\mu kT. \tag{19}$$

Based on the determined value of γ_p, for *m*-LPPP we deduce a polaron diffusion coefficient $D_p=8.7\times10^{-9}\,\mathrm{cm^2\,s}$ and a mobility $\mu_p=1\times10^{-6}\,\mathrm{cm^2/V\,s}$ at 123 K. As expected, due to the absence of an external electric field in the PA and PLDMR measurements, the obtained mobility is much lower than mobilities obtained from time-of-flight measurements. For *m*-LPPP, a hole mobility $\mu_h=4\times10^{-4}\,\mathrm{cm^2/V\,s}$ was found at 123 K at a field of 4×10^4 V/cm.

The polaron-induced SE quenching rate constant γ_q is a measure of the interaction of SE's with polarons and it is related to the diffusivities of both the SE's and polarons. Yet Table I shows that $\gamma_q\gg\gamma_p$, which clearly indicates that highly mobile SE's are quenched at rather immobile polarons. In this context we emphasize that for all OLED applications polarons will move much faster since they are accelerated by an external electric field. However, for the theoretically calculated SE size $R\approx2$ nm,[50] the SE diffusion constant is $D_{\mathrm{SE}}=4\times10^{-4}\,\mathrm{cm^2/s}$ in *m*-LPPP. With $r=\sqrt{\tau D}$ and the lifetime $\tau\approx10^{-9}$ s, the mean diffusion length of SE's is $r\approx6$ nm. It was recently found the migration of SE's in *m*-LPPP decreases[31] by 50%–60% as T decreases from 300 to 20 K. Hence a diffusion length of $r\approx6$ nm determined at 20 K is in excellent agreement with the room-temperature value of 15 nm obtained by Haugeneder *et al.* using a different technique,[51] and it demonstrates that the SE's are indeed more mobile than polarons. Therefore one would expect the PLDMR signal to increase with T as well since the interaction of polarons and SE increases. However, increasing T decreases the spin-lattice relaxation time T_1 and the number of trapped polarons, as PA (Ref. 8) and TSC (Ref. 16) measurements show, resulting in a PLDMR which decreases with T. Note that for LOPP7 one finds a diffusion radius of 4.3 nm at 20 K.

It should also be noted that a calculation of the magnetic resonance-induced change in n_p vs N_0 as observed by PADMR predicts a sublinear increase with N_0, in complete agreement with the behavior observed in Fig. 5.

We recently found[16] that the density of trapped polarons, n_p, determined from PLDMR and the number of trap states determined from TSC are much higher in the amorphous *m*-LPPP, where $n_p\geqslant1.6\times10^{16}\,\mathrm{cm^{-3}}$, than in polycrystalline parahexaphenyl (PHP), where $n_p\geqslant1.4\times10^{14}\,\mathrm{cm^{-3}}$. Hence both signals are proportional to the number of trapped polarons, n_p. Furthermore, it was found that upon photooxidation one increases the density of carbonyl groups,[34] which in turn increases the steady-state density of polarons as observed by PA (Ref. 26) and, consistent with the model presented in this work, the amplitude $\Delta I_{\mathrm{PL}}/I_{\mathrm{PL}}$ of the polaron PLDMR.[26]

The present study shows that the interaction between SE's and polarons becomes a dominant nonradiative recombination process when $\gamma_q n_p\approx k_r$. Since one finds $\sim10^{17}\,\mathrm{cm^{-3}}$ trap sites to stabilize polarons in this class of materials at high N_0, the nonradiative quenching will lead to a drastic reduction of the quantum yield and the observation of a sublinear dependence of I_{PL} on the excitation densities. Such behavior has indeed been observed,[52] but it was assigned to bimolecular SE-SE annihilation. However, the present analysis suggests that SE quenching by polarons will lead to the same behavior. Hence this interaction must be considered in future analysis of such sublinear behavior.

For OLED's at high driving currents yielding polaron densities of order $10^{18}\,\mathrm{cm^{-3}}$,[18] the absence of net optical gain was attributed to the strong polaron-induced absorption in their emission region. Taking into account the effect of SE-polaron quenching means that to obtain net optical gain in an electrically pumped organic laser one has to spatially separate the transport and emissive media in order to avoid the interaction of polarons and SE's.

V. CONCLUSION

In conclusion, a quantitative analysis of the nonradiative quenching of singlet excitons by polarons was accomplished by combining experimental excitation density-dependent photoluminescence (PL), PL-detected magnetic resonance (PLDMR), photoinduced absorption (PA), and PA-detected magnetic resonance (PADMR) with a new rate equation model. The model described the behavior and the basic interaction of polarons and singlet excitons (SE's) in all four

experiments with one set of parameters. It is also in quantitative agreement with results of other studies, such as thermally stimulated current (TSC), SE diffusivity measurements, and extensive theoretical studies. The results show that the interaction of SE's with polarons becomes a dominant nonradiative recombination process when the quenching constant, which is a product of the polaron density n_p and the interaction parameter γ_q between SE's and polarons, becomes comparable to the radiative decay constant, i.e., $\gamma_q n_p \approx k_r$. In the class of materials described in this work, a strong quenching of SE's appears to occur at polaron densities of $\sim 10^{17}\,\mathrm{cm}^{-3}$. Since such polaron densities can be easily achieved upon photoexcitation or carrier injection, this study is relevant both for understanding the photophysics of conjugated polymers as well as for practical organic light-emitting device applications.

ACKNOWLEDGMENTS

The authors would like to thank J. Partee, E. L. Frankevich, and E. Zojer for valuable contributions. This work was supported by FWF P. #12806, BMWV, and by the Director for Energy Research, Office of Basic Energy Sciences, U.S. Department of Energy (U.S. DOE). Ames Laboratory is operated by Iowa State University for the U.S. DOE under Contract No. W-7405-Eng-82.

*Author to whom correspondence should be addressed. Electronic address: e.list@tugraz.at

†Present address: eMagin Corporation, Hopewell Junction, New York 12533.

[1] S. Tasch, A. Niko, G. Leising, and U. Scherf, Appl. Phys. Lett. **68**, 1090 (1996).

[2] C. Zenz, W. Graupner, S. Tasch, G. Leising, K. Müllen, and U. Scherf, Appl. Phys. Lett. **71**, 2566 (1997); S. Stagira, M. Zavelani-Rossi, M. Nisoli, S. DeSilvestri, G. Lanzani, C. Zenz, P. Mataloni, and G. Leising, *ibid.* **73**, 2860 (1998); B. Schweitzer, G. Wegmann, D. Hertel, R. F. Mahrt, H. Bässler, F. Uckert, U. Scherf, and K. Müllen, Phys. Rev. B **59**, 4112 (1999).

[3] S. Tasch, G. Kranzelbinder, G. Leising, and U. Scherf, Phys. Rev. B **55**, 1 (1997).

[4] W. Graupner, S. Eder, M. Mauri, G. Leising, and U. Scherf, Synth. Met. **69**, 419 (1995).

[5] M. G. Harrison, S. Müller, G. Weiser, G. Urbasch, R. F. Mahrt, H. Bässler, and U. Scherf, Phys. Rev. B **60**, 8650 (1999).

[6] W. Graupner, G. Cerullo, G. Lanzani, M. Nisoli, S. De Silvestri, E. J. W. List, and G. Leising, Phys. Rev. Lett. **81**, 3259 (1998).

[7] V. I. Arkhipov, E. V. Emelianova, and H. Bässler, Chem. Phys. Lett. **296**, 452 (1998); B. Schweitzer, V. I. Arkhipov, and H. Bässler, *ibid.* **304**, 365 (1999).

[8] M. Wohlgenannt, W. Graupner, G. Leising, and Z. Vardeny, Phys. Rev. Lett. **82**, 3344 (1999).

[9] M. Wohlgenannt, W. Graupner, G. Leising, and Z. Vardeny, Phys. Rev. B **60**, 5321 (1999).

[10] W. Graupner, T. Jost, K. Petritsch, S. Tasch, G. Leising, M. Graupner, and A. Hermetter, Soc. Plastics Engineers, Technical Papers **XLIII**, 1339 (1997).

[11] R. Kersting, U. Lemmer, R. F. Mahrt, K. Leo, H. Kurz, H. Bässler, and E. O. Göbel, Phys. Rev. Lett. **70**, 3820 (1993).

[12] D. D. C. Bradley and R. H. Friend, J. Phys.: Condens. Matter **1**, 3671 (1989); K. E. Ziemelis, A. T. Hussain, D. D. C. Bradley, R. H. Friend, J. Rühe, and G. Wegner, Phys. Rev. Lett. **66**, 2231 (1991).

[13] H. Antoniadis, L. J. Rothberg, F. Papadimitrakopoulos, M. Yan, M. E. Galvin, and M. A. Abkowitz, Phys. Rev. B **50**, 14911 (1994).

[14] W. Graupner, F. Meghdadi, G. Leising, G. Lanzani, M. Nisoli, S. De Silvestri, W. Fischer, and F. Stelzer, Phys. Rev. B **56**, 10128 (1997).

[15] P. A. Lane, X. Wei, and Z. V. Vardeny, Phys. Rev. Lett. **77**, 1544 (1996).

[16] E. J. W. List, C. H. Kim, J. Shinar, A. Pogantsch, G. Leising, and W. Graupner, Appl. Phys. Lett. **76**, 2083 (2000).

[17] J. H. Schön, C. Kloc, A. Dodabalapur, and B. Batlogg, Science **289**, 599 (2000).

[18] V. G. Kozlov, P. E. Burrows, G. Parthasarathy, and S. R. Forrest, Appl. Phys. Lett. **74**, 1057 (1999).

[19] W. Graupner, G. Leditzky, G. Leising, and U. Scherf, Phys. Rev. B **54**, 7610 (1996).

[20] X. Wei, B. C. Hess, Z. V. Vardeny, and F. Wudl, Phys. Rev. Lett. **68**, 666 (1992).

[21] Z. V. Vardeny and X. Wei, Mol. Cryst. Liq. Cryst. Sci. Technol., Sect. B **256**, 465 (1994); J. Shinar, Synth. Met. **78**, 277 (1996).

[22] V. Dyakonov and E. L. Frankevich, Chem. Phys. **227**, 203 (1998); V. Dyakonov, G. Rösler, M. Schwoerer, and E. L. Frankevich, Phys. Rev. B **56**, 3852 (1997).

[23] U. Scherf and K. Müllen, Makromol. Chem., Rapid Commun. **12**, 489 (1991).

[24] J. Grimme and U. Scherf, Makromol. Chem. **197**, 2297 (1996).

[25] W. Graupner, J. Partee, J. Shinar, G. Leising, and U. Scherf, Phys. Rev. Lett. **77**, 2033 (1996).

[26] E. J. W. List, J. Partee, J. Shinar, U. Scherf, K. Müllen, W. Graupner, and G. Leising, Phys. Rev. B **61**, 10807 (2000).

[27] CH. P. Poole, ESR: *A Comprehensive Treatise on Experimental Techniques* (Wiley, New York, 1983).

[28] M. Phelan *et al.* (unpublished).

[29] F. T. H. den Hartog, C. van Papendrecht, R. J. Silbey, and S. Völker, J. Chem. Phys. **110**, 1010 (1999).

[30] R. Kersting, U. Lemmer, R. F. Mahrt, K. Leo, H. Kurz, H. Bässler, and E. O. Göbel, Phys. Rev. Lett. **70**, 3820 (1993).

[31] E. J. W. List, C. Creely, G. Leising, N. Schulte, A. D. Schlüter, U. Scherf, K. Müllen, and W. Graupner, Chem. Phys. Lett. **325**, 132 (2000).

[32] Th. Förster, Ann. Phys. **2**, 55 (1948).

[33] E. J. W. List, C. H. Kim, W. Graupner, G. Leising, and J. Shinar, Synth. Met. **119**, 511 (2001).

[34] W. Graupner, M. Sacher, M. Graupner, C. Zenz, G. Grampp, A. Hermetter, and G. Leising, in *Electrical, Optical, and Magnetic Properties of Organic Solid-State Materials IV*, edited by J. R. Reynolds, A. K. Y. Jen, L. R. Dalton, M. F. Rubner, and L. Y. Chiang, Mater. Res. Soc. Symp. Proc. No. 488 (Materials Research Society, Pittsburgh, 1998), p. 789.

[35] M. Pope and C. E. Swenberg, *Electronic Processes in Organic Crystals* (Oxford University Press, New York, 1998).

[36] R. A. J. Janssen, L. Smilowitz, N. S. Sariciftci, and D. Moses, J. Chem. Phys. **101**, 1787 (1994).
[37] D. Hertel, H. Bässler, U. Scherf, and H. H. Hörhold, J. Chem. Phys. **110**, 9214 (1999).
[38] E. Zojer, J. Cornil, G. Leising, and J. L. Brédas, Phys. Rev. B **59**, 7957 (1999).
[39] W. Graupner, M. Mauri, J. Stampfl, G. Leising, U. Scherf, and K. Müllen, Solid State Commun. **91**, 7 (1994).
[40] Note that calculating the density of ground states assuming $N = \rho N_A / m_W$ does not account for the fact that the excited state has a size larger than the repeat unit.
[41] G. Kranzelbinder, W. Graupner, K. Müllen, U. Scherf, and G. Leising, Proc. SPIE **3145**, 48 (1997).
[42] U. E. Steiner and T. Ulrich, Chem. Rev. **89**, 51 (1989).
[43] E. J. W. List, W. Graupner, G. Leising, J. Partee, and J. Shinar, in *Electrical, Optical, and Magnetic Properties of Organic Solid-State Materials IV* (Ref. 34), p. 99.
[44] S. Irle and H. Lischka, J. Chem. Phys. **107**, 3021 (1997).
[45] Z. Shuai, D. Beljonne, R. J. Silbey, and J. L. Bredas, Phys. Rev. Lett. **84**, 131 (2000).
[46] M. Wohlgenannt, K. Tandon, S. Mazumdar, S. Ramasesha, and Z. V. Vardeny, Nature (London) **409**, 494 (2001).
[47] G. Kranzelbinder, H. J. Byrne, S. Hallstein, S. Roth, G. Leising, and U. Scherf, Phys. Rev. B **56**, 1632 (1997).
[48] E. J. W. List and W. Graupner (unpublished).
[49] D. A. dos Santos, D. Beljonne, J. Cornil, and J. L. Brédas, Chem. Phys. **227**, 1 (1998).
[50] D. Beljonne, Z. Shuai, R. H. Friend, and J. L. Brédas, J. Chem. Phys. **102**, 2042 (1995); D. Beljonne, J. Cornil, R. H. Friend, R. A. J. Janssen, and J. L. Brédas, J. Am. Chem. Soc. **118**, 6453 (1996); D. Beljonne, H. F. Wittmann, A. Köhler, S. Graham, M. Younus, J. Lewis, P. R. Raithby, M. S. Khan, R. H. Friend, and J. L. Brédas, J. Chem. Phys. **105**, 3868 (1996).
[51] A. Haugeneder, M. Neges, C. Kallinger, W. Spirkl, U. Lemmer, J. Feldmann, U. Scherf, E. Harth, A. Gügel, and K. Müllen, Phys. Rev. B **59**, 15346 (1999).
[52] G. J. Denton, N. Tessler, N. T. Harrison, and R. H. Friend, Phys. Rev. Lett. **78**, 733 (1997).